Extended Abstracts of the 2020 International Conference on Solid State Devices and Materials, VIRTUAL conference, 2020, pp333-334

Benchmark of Phase Modulators for high-speed and low power Integrated Optical Phased Array in 3D sensing Applications

C. Barrera[1,2,3], Y. Désières[2], D. Fowler[2], I. Charlet[1,2,3], L. Vivien[3], F. Boeuf[1]

[1] STMicroelectronics, Crolles, France ; [2] CEA-LETI ; [3] C2N CNRS Palaiseau

Abstract

In this paper, we review the performance trade-offs of Phase Modulator (PM) in typical silicon photonic platforms for the fabrication of integrated optical phased arrays (OPA) for 1550 nm-based LiDAR applications.

1. Introduction

With the development of automated driving and remote sensing technologies, light detection and ranging (LIDAR) has attracted great attention for future mass market deployment[1]. Optical phased arrays (OPA) based on silicon photonics have become an enticing solution for high-volume/low-cost LIDAR due to the absence of moving elements and the low unit costs associated with CMOS technology. Among the various devices that make up an integrated OPA, the phase modulator (PM) is perhaps that which has the greatest bearing on the overall circuit performance. Widely studied for telecommunications applications [2], this device actively modifies the effective refractive index of a waveguide via the thermo-optical (TO) [3] or free-carrier dispersion effects (FCD)[4]. In OPAs, PMs act on a multitude of individual waveguides to control to the output beam angle (Fig.1). Consequently, their energy efficiency, insertion loss, and bandwidth have a critical influence on the performance of the OPA.

2. OPA architecture

Whether we focus on mobile or automotive applications, specifications combined to our OPA analytical models predict the need of around 1k antennas with a pitch/λ ratio around 1 to guarantee a proper beam divergence (Fig.2). Such antenna numbers affects individual PM consumption target, especially when total consumption (laser source + OPA + detector) is limited to few 100s of mW (mobile application) to 10 W (automotive). Therefore, each PM shall not consume over 1 mW in such large-scale OPA. Framerate, number of points and switching time requires also 1 MHz bandwidth. While TO-PMs are the most widely used into OPAs due to their limited length and losses, they are intrinsically too slow and power hungry for such applications (Fig.3), with speed below 100 kHz and power consumption around 1~10 mW in the best cases. Although higher speeds are accessible through FCD PMs, they suffer from higher insertion losses due to free carrier absorption.

3. Low-power phase modulators

If carrier-injection based PIN diode can be efficient, then can hardly consume below 1 mW due to the high level of current (1mA for 1V)[5]. However, PN junction and SISCAP are respectively based-on carrier depletion and accumulation mechanisms and are intrinsically low power and extremely fast. Typical insertion losses seems incompatible for OPA firstly because those devices were previously designed for telecommunications with high doping levels to improve bandwidth at the cost of consistent insertion losses. Consequently, there still many optimization work to minimize losses.

We discuss here how to design PN and SISCAP from previous telecommunication architectures [6], [7] (Fig.4) to new friendly-OPA parameters. We use here combination of an analytic OPA model, electro-optical simulation using Lumerical software, fabrication-induced loss values from literature [2], [6], and the assumption of a continuously scanning OPA, supplied from 0 to 3.3V to respect typical power supply values. We plot both bandwidth, PM length and the OPA output-beam attenuation due to the variable optical losses. Although optimization of those devices is highly multi-parametric, we focus here on the doping level for the PN junction and thickness oxide (EOT) for the SISCAP. For PN, Fig.5 shows that doping higher than $10^{17}cm^{-3}$ increases attenuation while very-low doping gives good transparency at the expense of an increased device length. For a scattering loss of 1dB/cm, A 17mm optimum device length is found for a doping of n=p=5 10^{16} cm^{-3} with a still sufficient bandwidth for 3D sensing applications. However, those lengths make it critically dependent from fabrication-induced loss and its control becomes strategic to reduce the attenuation.

To reduce length and fabrication dependence, SISCAP is an alternative because carrier accumulation is more efficient than depletion, mainly at the expense of bandwidth. We keep a 5 $10^{16}cm^{-3}$ doping as a comparison tool with PN and we vary the EOT. As upper layer is made by poly-Si, expected propagation losses averaged at 4.5 dB/cm are much higher than PN. However, Fig.6 shows thinner EOT yields lower beam attenuation over much shorter device. This solution seems better than PN because length is improved, attenuation is similar but fabrication dependence is lowered. Bandwidth, although highly lowered, remains competitive.

To outperform those losses values of 2-3 dB, a promising solution for SISCAP is to replace the n-poly-Si by an n-InGaAsP material[9], with higher calculated carrier-induced change in refraction over attenuation [9] (Fig.7 & 8). Same simulations than Fig.6 are operated with III-V/Si SISCAP in Fig.9, we see the same behaviours, and exception made than

attenuation is below 0.5 dB and length below 500 μm, even shorter than TO-PMs but much faster and low-power.

4. Conclusion

We demonstrate that PN and SISCAP phase modulators are a promising way to build fast and low power OPAs for LiDARs application. If we have to combine all the advantages, hybrid III-V/Si SISCAP appears as the best solution. However, difficult integration techniques are required to benefit from this superiority. In addition, such hybrid modulators are limited in the field of silicon transparency (> 1.1 µm) and LiDARs based on 905-940 nm are still awaiting for such low power phase modulators.

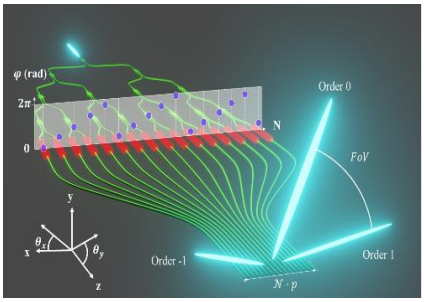

Figure 1: OPA architecture with passives (green), PM (red) and phase distribution (blue)

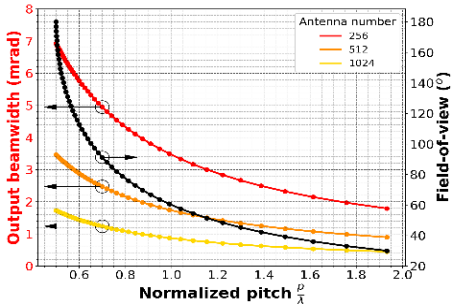

Figure 2: laser beam width (left) and field-of-view (right) with antennas' spacing and number.

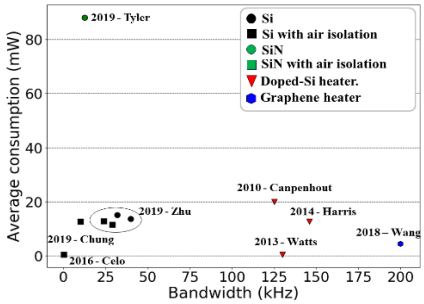

Figure 3: state-of-the art thermal phase shifters with various architectures and materials.

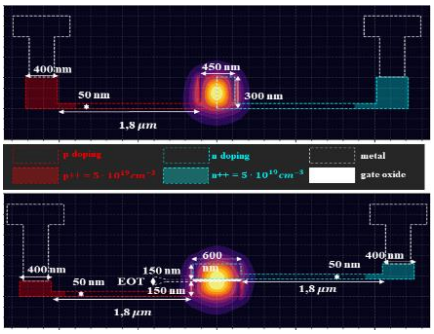

Figure 4: PN (top) and SISCAP (bottom) fixed and variable parameters (n, p, EOT) for numerical simulations.

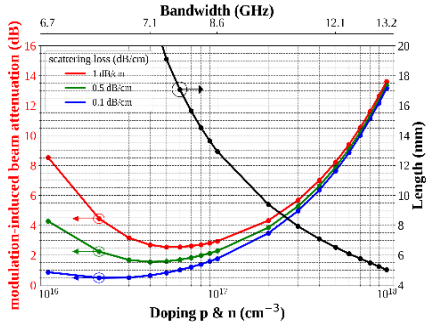

Figure 5: Evolution of PN's length, beam-attenuation and bandwidth with doping level.

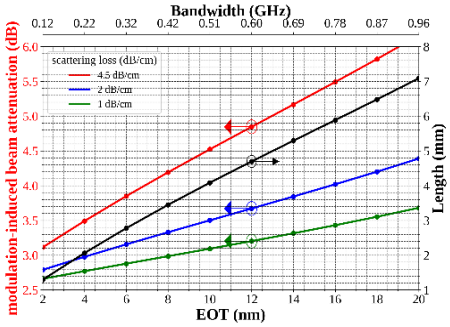

Figure 6: Evolution of pure-Si SISCAP's length, beam-attenuation and bandwidth with EOT.

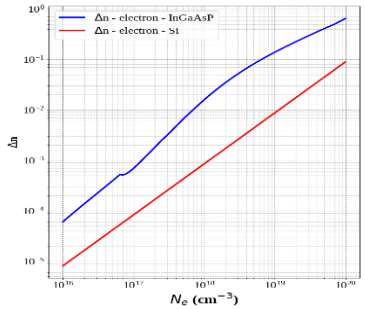

Figure 7: Carrier-induced change in refractive index for n-Si (red) and n-$In_{0.69}Ga_{0.31}As_{0.7}P_{0.3}$ (blue).

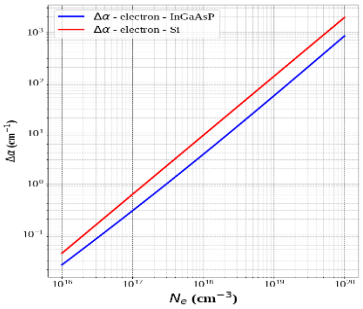

Figure 8: Carrier-induced change in absorption coefficient for n-Si (red) and n-InGaAsP (blue).

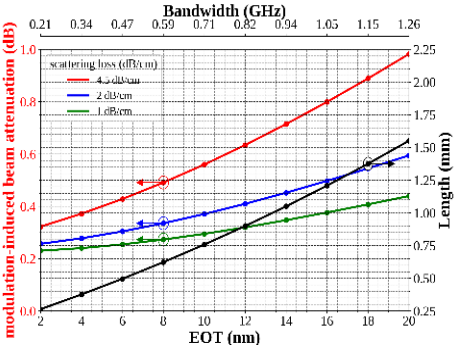

Figure 9: Evolution of Si/III-V SISCAP's length, beam-attenuation and bandwidth with EOT.

References

[1] M. J. R. Heck, *Nanophotonics*, vol. 6, no. 1, pp. 93–107, Jan. 2017
[2] F. Boeuf *et al.*, *2019 IEEE International Electron Devices Meeting (IEDM)*, 2019, pp. 33.1.1-33.1.4
[3] Di Ricercaper, *Sensors and Actuators*, vol. A, no. 71, pp. 19–26, 1998.
[4] M. Nedeljkovic, R. Soref, and G. Z. Mashanovich, *IEEE Photonics Journal*, vol. 3, no. 6, pp. 1171–1180, Dec. 2011
[5] G. Kang *et al.*, *IEEE Photonics Technology Letters*, vol. 31, no. 21, pp. 1685–1688
[6] M. Douix *et al.*, *Opt. Express, OE*, vol. 26, no. 5, pp. 5983–5990, Mar. 2018
[7] S. Monfray *et al.*, *Integrated Photonics Platforms: Photonics Europe, Fundamental Research, Manufacturing and Applications*, Apr. 2020, vol. 11364, p. 1136403
[8] J.-H. Han et al., *Nature Photonics*, vol. 11, no. 8, pp. 486–490, Aug. 2017
[9] B. R. Bennett et al., *IEEE Journal of Quantum Electronics*, vol. 26, no. 1, pp. 113–122, 1990